Available online at www.sciencedirect.com
SCIENCE DIRECT
Bioorganic & Medicinal Chemistry Letters
Bioorganic & Medicinal Chemistry Letters 16 (2006) 2037–2041

Factor VIIa inhibitors: Chemical optimization, preclinical pharmacokinetics, pharmacodynamics, and efficacy in an arterial baboon thrombosis model

Wendy B. Young,[a,*] Joyce Mordenti,[a] Steven Torkelson,[a] William D. Shrader,[a] Aleksandr Kolesnikov,[a] Roopa Rai,[a] Liang Liu,[a] Huiyong Hu,[a] Ellen M. Leahy,[a] Michael J. Green,[a] Paul A. Sprengeler,[a] Bradley A. Katz,[a] Christine Yu,[a] James W. Janc,[a] Kyle C. Elrod,[a] Ulla M. Marzec[b,†] and Stephen R. Hanson[b,†]

[a]*Celera Genomics, 180 Kimball Way, South San Francisco, CA 94080, USA*
[b]*Emory University, Atlanta, GA 30322, USA*

Received 5 October 2005; revised 13 December 2005; accepted 15 December 2005
Available online 18 January 2006

Abstract—Highly selective and potent factor VIIa–tissue factor (fVIIa·TF) complex inhibitors were generated through structure-based design. The pharmacokinetic properties of an optimized analog (**9**) were characterized in several preclinical species, demonstrating pharmacokinetic characteristics suitable for once-a-day dosing in humans. Analog **9** inhibited platelet and fibrin deposition in a dose-dependent manner after intravenous administration in a baboon thrombosis model, and a pharmacodynamic concentration–response model was developed to describe the platelet deposition data. Results for heparin and enoxaparin (Lovenox®) in the baboon model are also presented.

The activated factor VIIa–tissue factor (fVIIa·TF) complex has been shown to play a key role in blood coagulation. Accordingly, much research has focused on the generation of small molecule inhibitors of the fVIIa·TF complex as effective and potentially safer anti-thrombotic agents.[1] We have previously reported on the development of small molecule inhibitors of the fVIIa·TF complex.[1a,1b] Herein, we describe the continued optimization of the 2-[5-(5-carbamimidoyl-1*H*-benzoimidazol-2-yl)-5′-fluoro-6,2′-dihydroxy-biphenyl-3-yl] succinic acid scaffold (**1**)[1b] (Table 1). The preclinical pharmacokinetics, pharmacodynamics, and in vivo efficacy of lead analog **9** in a baboon arterial thrombosis model are the focus of this communication.

To continue in the optimization of our fVIIa·TF inhibitor series, we realized that the next goal was to improve the ex vivo efficacy as monitored by the PT (prothrombin time) assay.[2] While working toward this goal, we also aimed to maintain high selectivity (>1000-fold) for fVIIa versus related enzymes such as factor Xa (fXa) and factor IIa (fIIa).[3] Although compound **1** demonstrated excellent selectivity and potency for the purified enzyme system (fVIIa·TF $K_i = 0.004\ \mu M$), the ex vivo efficacy in human plasma was rather poor ($2\times$ PT = 10.2 μM). As it is generally well accepted that lowering binding to serum albumin will improve the results in the PT assay, we aimed to generate more polar and water-soluble analogs to decrease protein binding. Additionally, further increases in potency for fVIIa·TF would lead to improved ex vivo efficacy.

A crystal structure of **1** in fVIIa·TF revealed that the trajectory off the *para* position to the C-ring hydroxyl offers a large pocket that provides access to Lys60A and Asp60, as well as the backbone of His57.[1b] It was anticipated that we could improve binding to fVIIa by incorporating moieties that bind to such residues. In this process, incorporation of increasingly polar moieties

Keywords: Factor VIIa; fVIIa; Tissue factor; TF; Coagulation; Antithrombotic; Baboon thrombosis model; Pharmacokinetics; Pharmacodynamics; Serine protease; Thrombin; Factor Xa.
* Corresponding author. E-mail: wendy.young@yahoo.com
† Present address: Oregon Health and Science University, OGI School of Science and Engineering, 20000 NW Walker Road, Beaverton, OR 97006, USA.

0960-894X/$ - see front matter © 2006 Elsevier Ltd. All rights reserved.
doi:10.1016/j.bmcl.2005.12.059

Table 1. SAR exploring the *para* position on the C-ring phenol

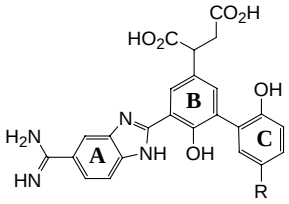

Compound	R	VIIa·TF K_i (μM)	Selectivity for fVIIa·TF versus		2× PT (μM)
			Xa[a]	IIa[b]	
1	F	0.004	1800	55,500	10.2
2	CO_2H	0.043	300	3500	8.2
3	CH_2CO_2H	0.012	125	12,500	6.2
4	$CH_2CH_2CO_2H$	0.013	350	11,500	5.4
5	$CONH_2$	0.014	1100	10,700	3.6
6	CH_2CONH_2	0.012	280	12,500	6.4
7	$NHCONH_2$	0.044	270	3400	4.9
8	CH_2NH_2	0.035	510	4200	2.9
9	$CH_2NHCONH_2$	0.002	3600	>100,000	1.9

[a] fXa K_i (μM)/fVIIa·TF K_i (μM) = fold selectivity.
[b] fIIa K_i (μM)/fVIIa·TF K_i (μM) = fold selectivity.

would also improve the ex vivo coagulation efficacy. Toward this end, we generated a series of analogs as depicted in Table 1. Based upon our X-ray structures, the succinic acid moiety extends into solvent, and the chirality was predicted to have minimal effect on binding potency. All analogs were generated and evaluated as a racemic mixture.

Analogs **2**–**4** were generated to potentially interact with Lys60A (or Lys192) via a salt bridge. While we did not improve binding to the protein with these analogs, as compared to **1**, it was encouraging to see that the ex vivo clotting values were improving. Similarly, extension of an amide into this region, as in analogs **5**–**6**, as well as the urea **7** and benzyl amine **8** did not offer any binding advantage, but the 2× PTs were again improved by the increased polarity of these analogs. Next, we extended the urea out by one methylene unit, producing **9**, the most potent compound in the series. Compound **9** was two times more active than **1** and had an improved 2× PT of 1.9 μM.

Compound **9** was evaluated against additional serine proteases, as well as a panel of biochemical assays in order to obtain a more complete selectivity profile. The compound was highly selective (>1000-fold) versus fXa, fIIa, trypsin, plasmin, uPa, aPC, tPa, and, hepsin and showed moderate selectivity ($\geqslant$100-fold) against factors IXa and XIa. It was essentially equipotent toward plasma-kallikrein. The 2× aPTT of analog **9** in human plasma is 0.8 μM. The potency of this analog in this assay is attributed to its plasma kallikrein activity. Analog **9** was tested for inhibition against five cytochrome P450 isozymes (1A2, 2C9, 2C19, 2D6, and 3A4), and inhibition was <40% at 10 μM. Additionally, analog **9** showed no alerts in a preliminary screen against 26 primary molecular targets[4] and was negative in the Ames test.[5]

A crystal structure of **9** in fVIIa·TF (Fig. 1)[6] revealed that the urea was indeed making contact with His57. A hydrogen bond was observed between the His57 carbonyl and the proximal aminomethyl NH of the inhibitor. The Lys60A donates an H-bond to the urea carbonyl perhaps contributing to the strength of the His57 interaction. This may account in part for the selectivity of the urea since fVIIa is the only enzyme with lysine in this position. The conformation of the carbonyl of His57 is also a likely contributor since in many enzymes it is involved in an intra-enzyme hydrogen bond or, as in trypsin, is pointed away from the ideal vector required for this interaction. The distal nitrogen of the urea is also involved in a hydrogen bond with Asp60.

The pharmacokinetic properties of **9** were evaluated after intravenous (IV) administration to C57BL/6 female mice, male Sprague–Dawley rats, male New Zealand White rabbits, male Beagle dogs, and male

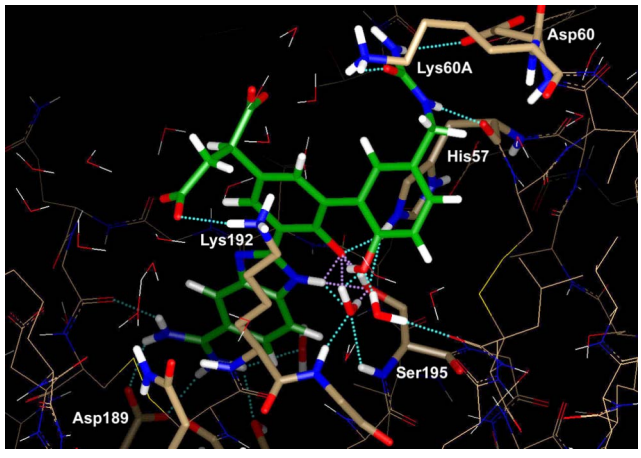

Figure 1. Crystal structure of analog **9** in fVIIa·TF complex.

baboons.[7] The pharmacokinetic parameters for plasma clearance (CL), volume of distribution at steady state (V_{ss}), and mean residence time (MRT) are provided in Table 2.

Preclinical pharmacokinetic data were extrapolated to humans using an allometric equation.[8] The allometric coefficient (*a*) and exponent (*b*) for each pharmacokinetic parameter are provided in Table 2, and the allometric relationship for CL is illustrated in Figure 2. From this analysis, plasma CL in a 70 kg human is predicted to be 147 mL/min, V_{ss} is predicted to be 71 L (or ~1 L/kg), and MRT is predicted to be 491 min (or ~8.2 h), which suggests once-a-day dosing in humans is possible.

The anti-thrombotic and anti-hemostatic effects of analog **9** were investigated in a baboon thrombosis model.[9] The ratio of the baboon-to-human prothrombin time (PT) for analog **9** was 1.05, indicating that it is near equipotent in both species. At single IV bolus doses of 0.03, 0.1, and 0.5 mg/kg (Fig. 3), analog **9** inhibited platelet deposition at 1 h post dose by 14%, 61%, and 87%, respectively, versus control animals (Table 3). Fibrin deposition was progressively reduced by increasing doses of **9**, similar to the results for platelet deposition.

Concurrently, PT values were prolonged 1.10-, 1.10-, and 1.13-fold over control values, respectively, while the bleeding time (BT) was slightly prolonged only at the highest dose (from 3.0 to 5.2 min) (Table 3). In comparison, standard doses of heparin (50 U/kg IV bolus plus 50 U/kg/h IV infusion) and enoxaparin (2 mg/kg subcutaneous administration) were also evaluated in this model and found to decrease platelet deposition by 77% and 62%, respectively, and to reduce fibrin deposition by 81% and 79%, respectively. These standard doses of heparin and enoxaparin increased the BT values by 1.9- and 2.1-fold over control values, respectively.

Table 2. Pharmacokinetics of **9** in preclinical species

Species	Weight (kg)	CL (mL/min)	V_{ss} (mL)	MRT (min)
Mouse	0.025	0.103	2.43	23.5
Rat	0.30	0.81	55.2	69.0
Rabbit	2.43	6.10	1080	182
Dog	11.3	30.5	6750	224
Baboon	11.5	26.5	5854	232
Allometric	*a*	2.84	285	102
Equation	*b*	0.93	1.3	0.37

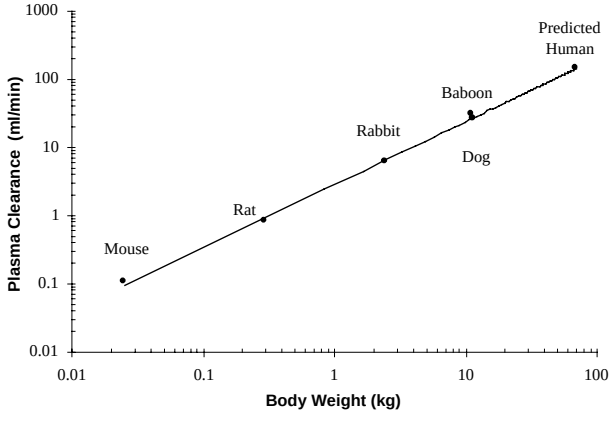

Figure 2. Interspecies scaling of **9** in mouse, rat, rabbit, dog, and baboon to predict the clearance in human.[8]

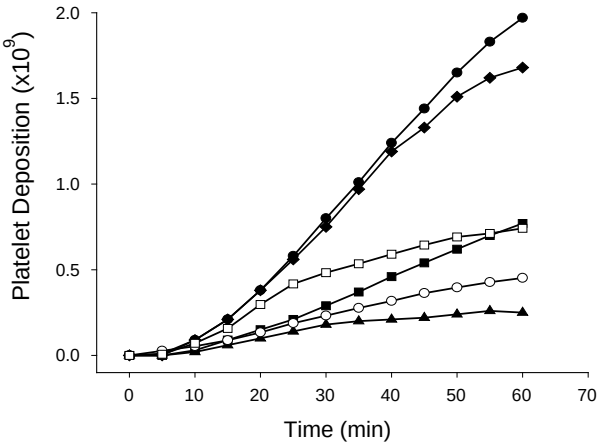

Figure 3. Effects of saline (control), analog **9**, heparin, and enoxaparin on platelet deposition in a baboon thrombosis model. Key: ● = saline control (n = 12); □ = enoxaparin (n = 3); ○ = heparin (n = 3); analog **9**: ♦ = 0.03 mg/kg (n = 3); ■ = 0.1 mg/kg (n = 4); ▲ = 0.5 mg/kg (n = 3).

Pharmacodynamic modeling[10] was used to determine the dose (milligrams per kilogram) and plasma concentration (micromolar) of analog **9** that were required to produce 50% of the maximum effect on platelets at 60 min post dose, that is, ED_{50} and EC_{50}, respectively. From this evaluation, the ED_{50} was 0.06 mg/kg, and the EC_{50} was 0.17 μM (Fig. 4).

To the best of our knowledge, this is the first report of a single IV bolus injection of a small molecule fVIIa·TF inhibitor to show complete inhibition of thrombus formation in a baboon model. Analog **9** appears to be approximately 50-fold more efficacious per weight basis than a previously studied small molecule inhibitor to fVIIa·TF, which required a IV bolus plus continuous IV infusion during the study period, using the same thrombosis model.[1d] There are reports of other selective small molecule fVIIa·TF inhibitors interrupting thrombosis in non-primate animal models, but these studies also required continuous infusion of drug.[1p]

All analogs were generated from compound **10** as outlined in Scheme 1. Starting from the commercially available 4-iodoanisole, the succinate moiety was inserted via a Heck reaction with subsequent catalytic hydrogenation to give **11**. This intermediate was then prepared for magnesium-directed *ortho* formylation by removing the methyl ether followed by re-esterification of the acid functions to produce **12**. After formylation, bromination, and boron ester formation, **13** underwent a Suzuki reaction with **14** to give product **15**. The remaining aldehyde group was the site for an oxidative-cyclization

Table 3. Inhibition of platelet and fibrin deposition, prothrombin time (PT), and bleeding times (BT) in baboon thrombosis model

Inhibitor (*n*/group)	Dose and route	Platelet deposition ± SD[a] platelets × 10^9 (% reduction vs control)	Fibrin deposition ± SD[a] mg fibrin/graft (% reduction vs control)	PT ± SD[a] (sec)	BT ± SD[b] (min)
Saline (12)	0 (control) IV	1.97 ± 0.58	1.77 ± 0.71	10.3 ± 0.8	3.0 ± 0.8
Analog **9** (3)	0.03 mg/kg IV	1.68 ± 0.24 (14)	1.41 ± 0.30 (20)	11.3 ± 0.7	3.2 ± 0.6
Analog **9** (4)	0.1 mg/kg IV	0.77 ± 0.47* (61)	0.63 ± 0.13* (64)	11.3 ± 0.5	3.8 ± 1.0
Analog **9** (3)	0.5 mg/kg IV	0.25 ± 0.27* (87)	0.25 ± 0.24* (86)	11.6 ± 0.6	5.2 ± 1.8*
Heparin[c](3)	50 U/kg bolus + 50 U/kg/h IV	0.45 ± 0.27* (77)	0.34 ± 0.28* (81)	NA	5.7 ± 1.3*
Enoxaparin[d] (3)	2 mg/kg SC	0.74 ± 0.43* (62)	0.38 ± 0.39* (79)	NA	6.3 ± 5.0*

NA = not available.
[a] 60 min after initiation of thrombosis.
[b] 30 min after initiation of thrombosis.
[c] American Pharmaceutical Partners, Schaunburg, IL.
[d] Lovenox® (Sanofi-Aventis SA).
* p versus control <0.05.

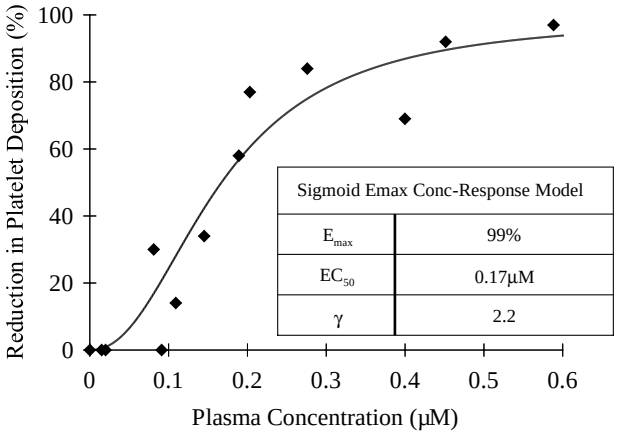

Figure 4. Pharmacodynamic model showing the plasma concentration of **9** versus reduction in platelet deposition in a baboon thrombosis model.[10]

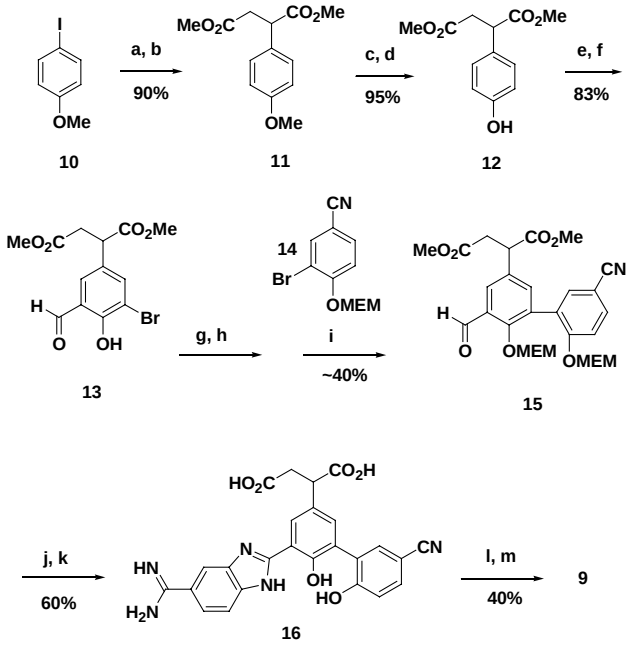

Scheme 1. Reagents and conditions: (a) dimethylfumarate, $PdCl_2$, NEt_3, MeCN; (b) $Pd(OH)_2/H_2$, MeOH; (c) HBr, reflux; (d) $SOCl_2$, MeOH; (e) paraformaldehyde, $MgCl_2$, TEA, MeCN; (f) *N*-bromosuccinimide, DMF; (g) MEM chloride, DIPEA, CH_2Cl_2; (h) KOAc, bis(pinacolato)diboron, dichloro[1,1′-bis-(diphenylphosphino)-ferrocene]palladiumII, dioxane; (i) $Pd(PPh_3)_4$, Na_2CO_3, toluene; (j) 3,4-diaminobenzamidine–HCl, O_2, EtOH; (k) 2 M HCl in dioxane then 1 M HCl at reflux; (l) $H_2/Pd(OH)_2$, 0.5 M HCl; (m) KOCN, water.

reaction to install the 5-amidinobenzimidazole moiety followed by the removal of the protecting groups. Finally, catalytic reduction of the nitrile group gave the corresponding amine, which was reacted with potassium cyanate to afford the crude product, which was purified by preparative HPLC to yield **9** as a racemic mixture.

In summary, highly potent and selective inhibitors of the fVIIa·TF complex were generated by structure-based design. The pharmacokinetics after IV dosing of lead analog **9** were evaluated in mouse, rat, rabbit, dog, monkey, and baboon. Allometric scaling predicts it could be suitable for once-a-day dosing in human. Compound **9** was found to be efficacious in an arterial baboon thrombosis model with an ED_{50} of 0.06 mg/kg and an EC_{50} of 0.17 μM after IV bolus dosing. At 0.5 mg/kg, it was more efficacious than standard doses of heparin and enoxaparin. Additionally, **9** did not impair hemostasis at the lower doses and was comparable to heparin and enoxaparin at the 0.5 mg/kg dose. These encouraging in vivo data provide additional support to our desire to develop fVIIa·TF inhibitors for improved anticoagulant therapy. Further advances in this chemical series will be reported in due time.

References and notes

1. (a) Young, W. B.; Kolesnikov, A.; Rai, R.; Sprengeler, P. A.; Leahy, E. M.; Shrader, W. D.; Sangalang, J.; Burgess-Henry, J.; Spencer, J.; Elrod, K.; Cregar, L. *Bioorg. Med. Chem. Lett.* **2001**, *11*, 2253; (b) Shrader, W. D.; Kolesnikov, A.; Burgess-Henry, J.; Rai, R.; Hendrix, J.; Hu, Huiyong; Torkelson, S.; Ton, T.; Young, W. B.; Katz, B. A.; Yu, C.; Tang, J.; Cabuslay, R.; Sanford, E.; Janc, J. J.; Sprengeler, P. A. *Bioorg. Med. Chem. Lett.*, in press; (c) Groebke Zbinden, K.; Banner, D. W.; Ackermann, J.; D'Arcy, A.; Kirchhofer, D.; Ji, Y.-H.; Tschopp, T. B.; Wallbaum, S.; Weber, L. *Bioorg. Med. Chem. Lett.* **2005**, *15*, 817; (d) Olivero, A. G.; Eigenbrot, C.; Goldsmith, R.;

Robarge, K.; Artis, D. R.; Flygare, J.; Rawson, T.; Sutherlin, D. P.; Kadkhodayan, S.; Beresini, M.; Elliott, L. O.; DeGuzman, G. G.; Banner, D. W.; Ultsch, M.; Marzec, U.; Hanson, S. R.; Refino, C.; Bunting, S.; Kirchhofer, D. *J. Biol. Chem.* **2005**, *280*, 9160; (e) Parlow, J. J.; Kurumbail, R. G.; Stegeman, R. A.; Stevens, A. M.; Stallings, W. C.; South, M. S. *J. Med. Chem.* **2003**, *46*, 4696; (f) Parlow, J. J.; Case, B. L.; Dice, T. A.; Fenton, R. L.; Hayes, M. J.; Jones, D. E.; Neumann, W. L.; Wood, R. S.; LaChance, R. M.; Girard, T. J.; Nicholson, N. S.; Clare, M.; Stegemann, R. A.; Stevens, A. M.; Stallings, W. C.; Kurumbail, R. G.; South, M. S. *J. Med. Chem.* **2003**, *46*, 4050; (g) Parlow, J. J.; Dice, T. A.; LaChance, R. M.; Girard, T. J.; Stevens, A. M.; Stegemann, R. A.; Stallings, W. C.; Kurumbail, R. G.; South, M. S. *J. Med. Chem.* **2003**, *46*, 4043; (h) Parlow, J. J.; Stevens, A. M.; Stegemann, R. A.; Stallings, W. C.; Kurumbail, R. G.; South, M. S. *J. Med. Chem.* **2003**, *46*, 4297; (i) Klingler, O.; Matter, H.; Schudok, M.; Bajaj, S. P.; Czech, J.; Lorenz, M.; Nestler, H. P.; Schreuder, H.; Wildgoose, P. *Bioorg. Med. Chem. Lett.* **2003**, *13*, 1463; (j) Carroll, A. R.; Pierens, G. K.; Fechner, G.; de Leone, P.; Ngo, A.; Simpson, M.; Hyde, E.; Hooper, J. N. A.; Bostreöm, S.-L.; Musil, D.; Quinn, R. J. *J. Am. Chem. Soc.* **2002**, *124*, 13340; (k) Hanessian, S.; Margarita, R.; Hall, A.; Johnstone, S.; Tremblay, M.; Parlanti, L. *J. Am. Chem. Soc.* **2002**, *124*, 13342; (l) Hanessian, S.; Therrien, E.; Granberg, K.; Nilsson, I. *Bioorg. Med. Chem. Lett.* **2002**, *12*, 2907; (m) Kohrt, J. T.; Filipski, K. J.; Rapundalo, S. T.; Cody, W. L.; Edmunds, J. J. *Tetrahedron Lett.* **2000**, *41*, 6041; (n) Jakobsen, P.; Horneman, A. M.; Persson, E. *Bioorg. Med. Chem.* **2000**, *8*, 2803; (o) Jakobsen, P.; Pedersen, B. R.; Persson, E. *Bioorg. Med. Chem.* **2000**, *8*, 2095; (p) Suleymanov, O. D.; Szalony, J. A.; Salyers, A. K.; Lachance, R. M.; Parlow, J. J.; South, M. S.; Wood, R. S.; Nicholson, N. S. *J. Pharmacol. Exp. Ther.* **2003**, *306*, 1115; (q) Roussel, P.; Bradley, M.; Kane, P.; Bailey, C.; Arnold, R.; Cross, A. *Tetrahedron* **1999**, *55*, 6219.

2. Bajaj, S. P.; Joist, J. H. *Semin. Thromb. Hemost.* **1999**, *25*, 407.
3. Inhibition assays for factor Xa and thrombin were performed as described (Cregar, L.; Elrod, K. C.; Putnam, D.; Moore, W. R. *Arch. Biochem. Biophys.* **1999**, *366*, 125,) with the pH adjusted to 7.4. Factor VIIa assay was performed and analyzed as above using 7 nM VIIa (Enzyme Research) and using CH_3SO_2-D-CHA-But-Arg-pNA (Centerchem) as the substrate. The buffer for the factor VIIa assay was supplemented with 11 nM relipidated tissue factor and 5 mM $CaCl_2$. Coagulation experiments were carried out in human plasma using a Beckman Coulter ACL100 in accordance with the manufacturer's instructions.
4. Analog **9** was evaluated in the HitProfilingScreen™ at MDS Pharma Services, Bothell, WA 98021.
5. Analog **9** was evaluated in the Ames Salmonella Mutagenicity Test with two mutant strains of *Salmonella typhimurium* LT2 (i.e., TA98 and TA100) with and without S9 activation at MDS Pharma Services, Taipei, Taiwan.
6. The PDB access code for the X-ray coordinates is 2B7D.
7. Plasma concentrations of **9** were assayed by LC/MS/MS. Pharmacokinetic data were analyzed by WinNonlin-Pro (Pharsight Corp.), using a two-compartment model.
8. The allometric equation is written as $Y = aW^b$, where Y is the pharmacokinetic parameter of interest, W is the body weight, a is the y-intercept, and b is the slope obtained from the plot of log Y versus log W (as illustrated in Fig. 2 for clearance parameter). See Mordenti, J. *J. Pharm. Sci.* **1986**, *75*, 1028, for details.
9. The animal experiments were approved by the Institutional Animal Care and Use Committee of Emory University in accordance with the United States federal guidelines. Thrombosis was initiated at a predetermined time after drug administration by interposing a thrombogenic device into a chronic femoral arterio-venous (A-V) shunt in conscious non-anticoagulated baboons. For analog **9** and heparin, thrombosis was initiated 5 min after IV bolus dosing (in the heparin group, an infusion continued throughout the experiment); whereas for enoxaparin, thrombosis was initiated 90 min after SC dosing. The thrombogenic device consisted of a 2 cm segment of porous expanded (poly)tetrafluoroethylene vascular graft (ePTFE, 4 mm id) filled with relipidated tissue factor. Blood flow was maintained at 100 mL/min, generating a wall shear rate of 265/s. Thrombus was monitored dynamically for 60 min by gamma camera imaging of autologous 111-indium (111-In)-labeled platelets. Images were acquired at 5 min intervals. Total platelet deposition was calculated at each time point by dividing the thrombus radioactivity (cpm) by the blood specific activity (cpm/mL) and multiplying by the blood platelet count (platelets/mL). Fibrin deposition was monitored by injecting a trace amount of 125-iodine (125-I)-labeled autologous fibrinogen 10 min before the start of the study, then saving the thrombus that formed in the graft for 30 days to permit decay of 111-In activity. The 125-I activity was measured in a gamma well counter. 125-I activity was converted to total deposited fibrin (mg) using values for the specific activity of plasma-clottable fibrinogen and the plasma fibrinogen concentration that were obtained at the time of the study. Template bleeding times (BT) were measured on a shaved forearm prior to dosing and at 30 min after initiation of thrombosis. The PT and aPTT were monitored throughout the study.
10. Dose (mg/kg) and plasma concentration (micromolar) versus response data were evaluated with a sigmoid E_{max} pharmacodynamic model, using WinNonlin-Pro (Pharsight Corp.). For plasma concentrations, the relationship has the general form $E = (E_{max} * C^{\gamma})/(C^{\gamma} + EC_{50}^{\gamma})$, where E = inhibition of platelet deposition (%) relative to control at 60 min post dose, E_{max} = maximum effect (%), C = plasma concentration of **9** at 60 min post dose, EC_{50} = plasma concentration of **9** required to produce 50% of the maximum effect, and γ = sigmoidicity or shape parameter. When dose (D) is evaluated, C is replaced by D (mg/kg) in the equation.